Journal of
NANOSTRUCTURES
JNS
NANOSTRUCTURES
JNS.kashanu.ac.ir

Synthesis of Cu Doped NiO Nanoparticles by Chemical Method

M. Aliahmad[a], A. Rahdar*[,b], Y. Azizi[a]

[a]*Department of Physics, Faculty of Science, University of Sistan and Baluchestan, Zahedan, Iran*

[b]*Departments of Physics, Faculty of Science, University of Zabol, Zabol, Iran*

Article history:
Received 12/2/2014
Accepted 27/4/2014
Published online 1/6/2014

Keywords:
Precipitation method
NiO:Cu
Nanoparticles
Hysteresis loop
VSM

**Corresponding author:*
E-mail address:
a.rahdar@uoz.ac.ir
Phone: +98 541 2446565
Fax: +98 542 2242503

Abstract

The Cu doped NiO (NiO:Cu) nanoparticles were synthesized by co-precipitation method using $NiCl_2.6H_2O$, $CuCl_2.2H_2O$ for Ni and Cu sources, respectively. Sodium hydroxide has been used as a precipitator agent. Effect of Cu doping agent on the structural and optical properties of nanostructures were characterized by XRD, SEM, AFM, spectrophotometry, FTIR and VSM techniques. XRD revealed that NiO:Cu has a FCC structure. Optical absorption spectra of the samples obtained using UV-Vis spectrophotometer shows a blue-shift when copper amount increase which indicates decreasing particle size. The study of magnetization property at room temperature shows weak ferromagnetic behavior of NiO:Cu nanoparticles. Hysteresis loops were show that magnetization increasing with Cu doping up to 13% and then with further doping decreasing.

1. Introduction

Over recent years increasing attention has been focused on the production of novel nanostructured metal oxide materials. One of the most commonly used transition metal oxides for a wide range of application is nickel oxide (NiO). It is a NaCl-type antiferromagnetic oxide semiconductor [1], which has attracted considerable attention for a range of applications; such as catalysts, electrochromic film, gas sensors, fuel cell, anode of organic light-emitting diodes, magnetic materials and thermoelectric materials, owing to its p-type conductivity, wide band gap ranging from 3.6 eV to 4.0 eV, excellent chemical stability, and electrical and optical properties [2–16]. Xiang et al. [17] prepared NiO nanoparticles with diameter of 10–15 nm by air-calcination of $Ni(OH)_2.NiCO_3.xH_2O$, while the agglomeration of nanoparticles is a difficult question from the SEM image. Wang et al. [18] prepared NiO nanocrystalline with average particle diameter of 18–55 nm using surfactant-mediated; however, from the transmission electron microscope image, the NiO nanoparticles were not well dispersed. Dongliang Tao et al. [19] prepared well-dispersed

NiO nanoparticles but the average particle diameter is 30 nm using polyvinylpyrrolidone assisted. Various other methods have been reported for the synthesis of NiO nanoparticles such as low-pressure spray pyrolysis [20], surfactant-mediated method [21], simple liquid phase process [22] and other techniques [23–24]. Among a range of methods for controlled synthesis, co-precipitation chemical route, based on solution process was used here to synthesize Cu doped NiO nanoparticles. Doping is a useful and effective process to change the structural, optical, electronic and magnetic properties of nanomaterials.

2. Experimental

2.1. Synthesis of NiO:Cu nanoparticles

NiO:Cu nanoparticles were prepared by the chemical co-precipitation method. $NiCl_2.6H_2O$, $CuCl_2.2H_2O$ and NaOH were purchased from Merck (Germany) with at least 99.0% purification. For NiO:Cu nanoparticles synthesis, in the first step, $NiCl_2.6H_2O$ and $CuCl_2.2H_2O$ (doping agent) were dissolved in double-distilled water which was acting as solvent to desired concentrations. Using a 0.1 molar each solutions different ratios of x = Cu/(Cu+Ni) (x = 0, 0.13 , 0.20) was prepared. Afterwards, 10 mL of NaOH (1M) was added drop wise to the solution. The resulting solution was magnetically stirred for 40 min at 50 ^oC temperature. In the final step, green precipitate was washed first with distilled water and then ethanol to remove any impurities such as the excess ions formed during the reaction process. Solid product was dried at 60 ^oC temperature for 14 h. Then, dried samples was calcinated at 500 ^oC temperature for 2 h to get NiO:Cu nanoparticles.

2.2. Materials characterization

X-ray diffraction patterns were taken by means of a Philips diffractometer model PW1800 (The Netherlands). X-ray source was Cukα with 1.541 nm wavelength. Scanning electron microscope (SEM) images and energy-dispersive x-ray spectroscopy (EDX) patterns were taken using VEGA\\TESCAN-XMU in Metallurgy Razi center. Atomic force microscope (AFM) observation was performed with Danish Micro Engineering (DME) Danish Micro Engineering (A/S DK-2730 Denmark). The experiments were carried out at room temperature in non-contact mode. UV-Vis spectra of the nanoparticles were obtained at room temperature using a PG (UK) instrument T80 UV-Vis spectrophotometer. Magnetization measurements were performed at room temperature using a vibrating sample magnetometer (MKD model-Iran). Infrared spectra were taken on a JASCO 640 plus infrared spectrometer in the range of 4000–4000 cm^{-1}.

3. Results and discussion

Fig. 1 shows X-ray diffraction pattern of the NiO:Cu nanoparticles with different doping percentages of Cu at room temperature. The mean crystallite size (D) of nanoparticles was also estimated using Scherer formula using (111) reflection from the XRD pattern as Eq. 1:

$$D = K\lambda/(\beta\cos\theta) \quad (1)$$

Where k is size factor (k = 0.9), λ is the wavelength (λ = 1.542 Å) (CuKα), β is the full width at half maximum (FWHM) of the peak, and θ is the diffraction angle. As seen in Fig. 1, all these diffraction peaks accordance with that of standard spectrum (card No. 01-073-1523, 01-078-0646 and 01-078- 0648) for x = 0, x = 0.13 and x = 0.20 samples, respectively. The Bragg peaks were obtained at 2θ values of 37, 43, 63, 75

and 79 degree correspond to (111), (200), (220), (311) and (222) planes for x = 0 samples, respectively. The peaks are obtained at 2θ values of 37.50 and 37.53 degree correspond to (111) plane for x = 0.13 and x = 0.20 samples, respectively. Peaks related to high angles due to the large line broadening have submerged in the background, which is attributed to the material nanoscale size. The average size of the x = 0.00, x = 0.13 and x = 0.20 samples obtained using (XRD) pattern at 26, 23 and 17 nm, respectively. The nanoparticles of x = 0.20 sample showed stronger peak intensity than samples of x = 0 and x = 0.13 indexing to the (111) plane which is pointed to improving crystallinity of NiO:Cu nanoparticles. Table 1 shows data of X-ray diffraction (XRD) pattern from the x = 0.13 samples after calcination.

The EDX spectra of the samples are shown in Fig. 2 and Fig. 3, which confirm presence of Ni, O and Cu elements as the only elementary species in the samples. No any additional peaks were observed. Also, the EDX spectrum of the samples shows that Cu peak intensity increase as doping concentration level increase.

Fig. 4 and Fig. 5 show the scanning electron microscopy (SEM) images of NiO:Cu nanoparticles with magnification of 5000 after calcination. The results indicate some of these particles have a spherical shape but agglomerations of particles are occurred. It is necessary to keep in mind that the observation of some larger nanoparticles may be attributed to the fact that NiO:Cu nanostructures due to their high surface energy and tension have the tendency to agglomeration. The average size of the x = 0.00 and x = 0.13 samples observed from SEM images is 23 and 19 nm, respectively.

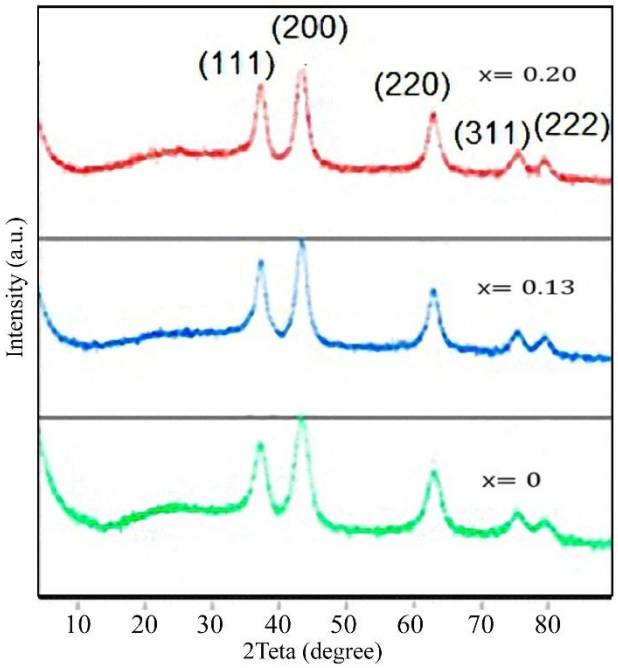

Fig. 1. XRD patterns of Cu-doped NiO nanoparticles after calcination.

Table 1. Data of X-ray diffraction (XRD) pattern of the x = 0.13 samples after calcination.

hkl	Position (2θ; degree)	FWHM (degree)	Peak height	Relative intensity
111	37.5052	0.7085	482.81	60.05
200	43.1884	0.3936	691.50	100.00
220	62.6797	0.3149	339.51	42.57
311	75.6702	1.1520	103.27	11.39
222	79.6915	0.3149	83.32	9.19

Fig.6 shows the atomic force microscopy (AFM) image of NiO:Cu nanoparticles before calcination. AFM images were obtained by measurement of the interaction forces between the tip and the sample surface. The average particle size of the x = 0.20 sample observed from AFM image is less than 54.3 nm.

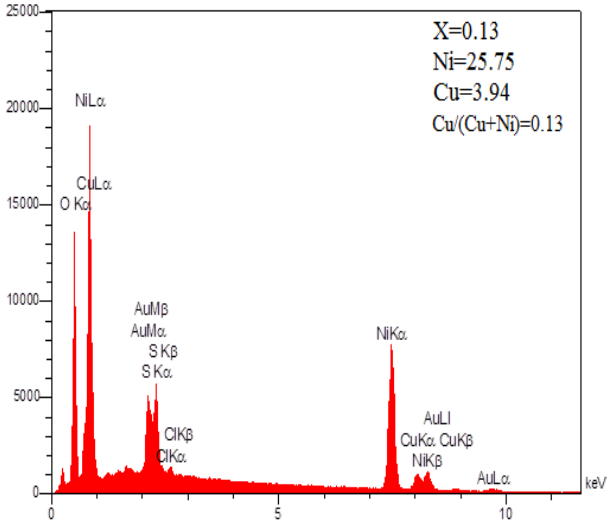

Fig. 2. EDX spectrum of x = 0.00 sample after calcination.

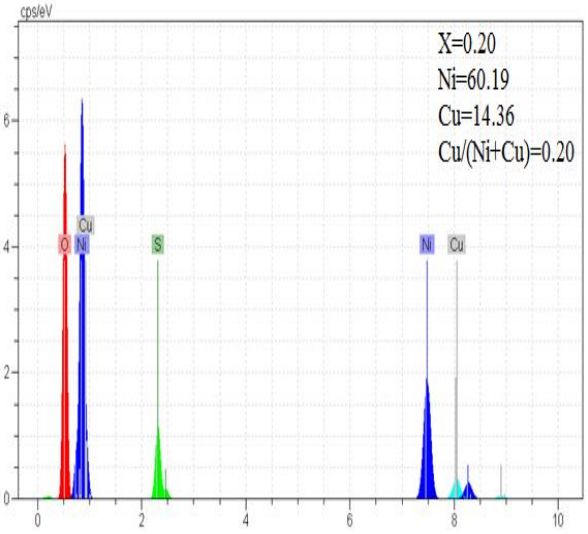

Fig. 3. EDX spectrum of x = 0.20 sample after calcination.

Magnetization measurements of NiO:Cu nanoparticles were performed using VSM technique and hysteresis loops of the samples at fields of -8000 to 8000 Oe at room temperature are shown in Fig. 7, Fig. 8 and Fig. 9 confirm that Hysteresis loops corresponding to these nanoparticles have superparamagnetic properties, which means magnetic remanence (Mr) and coercive force (Hc) are zero or very small. The values magnetic field [H] and magnetization [M] of samples are listed in Table 2.

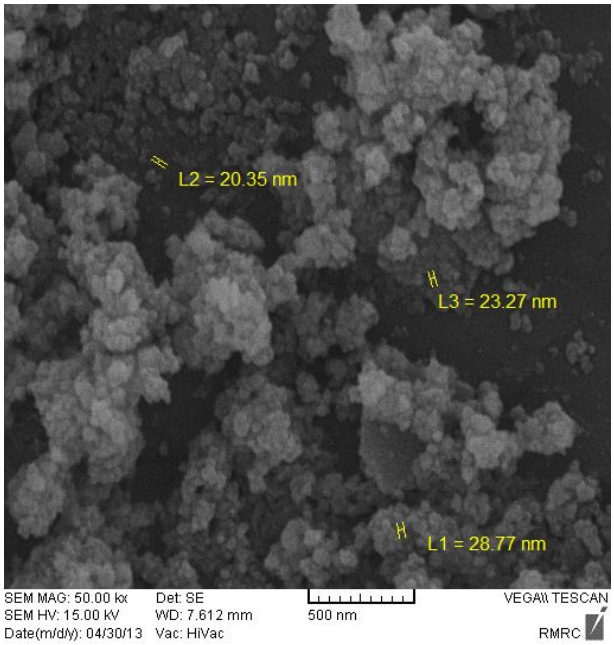

Fig. 4. SEM image of x = 0.00 sample after calcination.

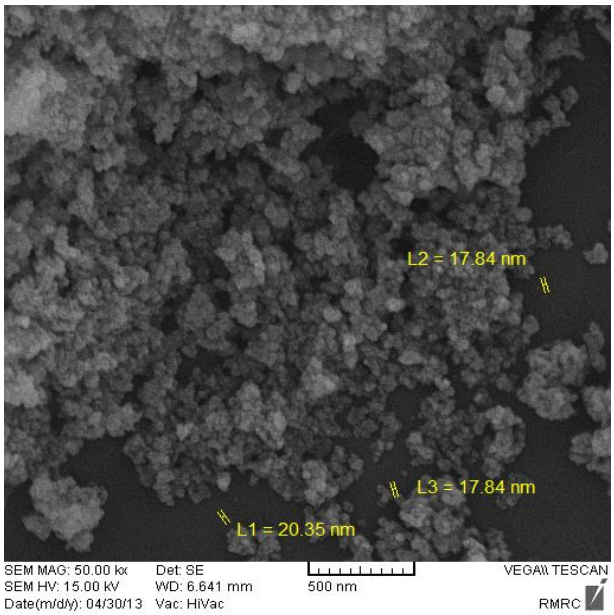

Fig. 5. SEM image of x = 0.13 sample after calcination.

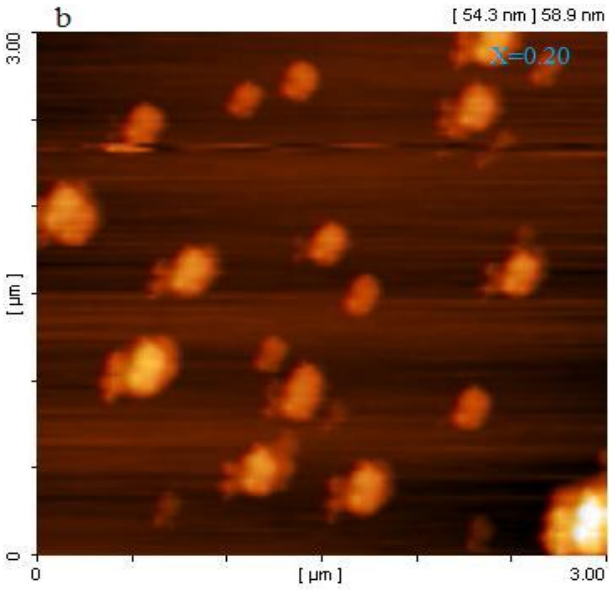

Fig. 6. AFM images of x = 0.20 sample before calcination.

This complex magnetic behaviour can be explained as follow. When the concentration of Cu doping agent is increased more than 13%, they are mediated by F-centre exchange coupling (FCE) interactions due the small separation between Cu ions, which result increase of magnetization with Cu contents. However, further increase in Cu ions may results super-exchange interactions between Cu ions mediated by oxygen ions. This super-exchange interaction results antiferromagnetic ordering, which reduce the ferromagnetic ordering in the NiO:Cu nanoparticles. The observed ferromagnetic behavior of NiO:Cu nanoparticle has been explained in the light of F-centre exchange coupling (FCE). Ferromagnetic room temperature in Cu doped NiO indicates that there is a competition between the FCE coupling and super-exchange coupling [25].

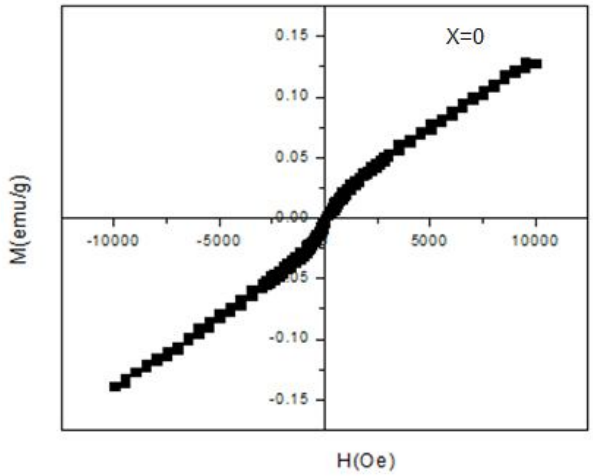

Fig. 7. M-H curve of x = 0.00 sample after calcination.

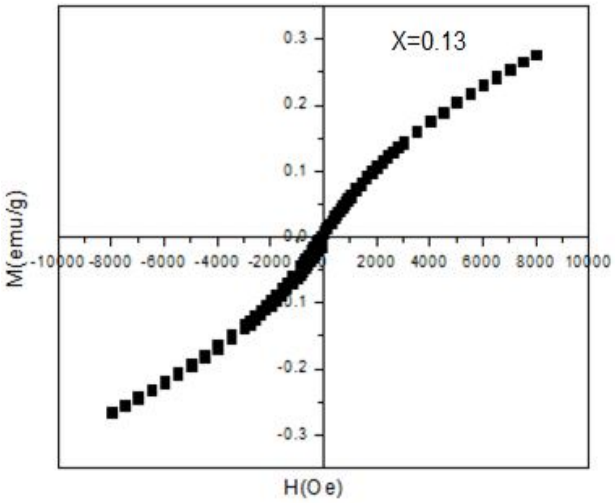

Fig. 8. M-H curve of x = 0.13 sample after calcination.

Fig. 10. shos the Magnetic hysteresis curves of Cu-doped NiO nanoparticles before calcination. As seen in Fig. 10, all of the samples have antiferromagnetism property before calcinations due to their weak ferromagnetism susceptibility

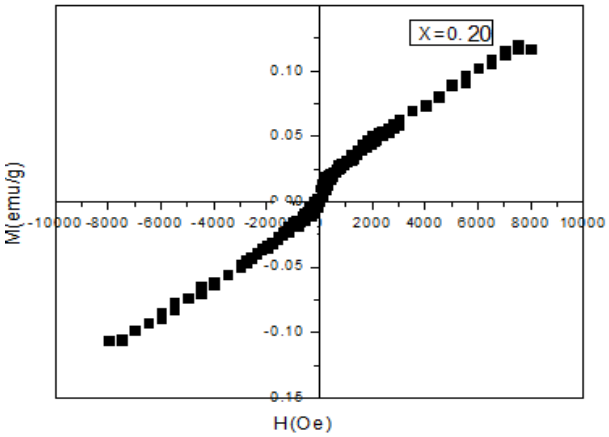

Fig. 9. M-H curve of x = 0.20 sample after calcination.

Table 2. Magnetization of samples with various amount of cupper before and after calcinations.

Sample	M (emu/g) before calcination	M (emu/g) after calcination	H_c Oe)
x = 0.00	0.32382	0.11076	8000
x = 0.13	0.91295	0.27751	8000
x = 0.20	0.55861	0.11675	8000

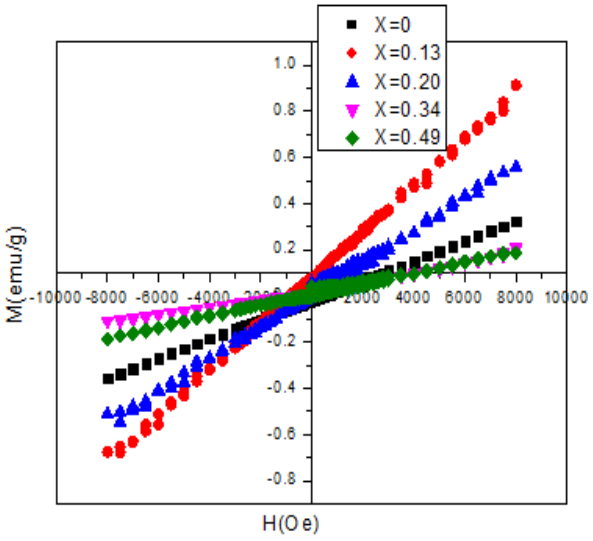

Fig. 10. M-H curves of Cu-doped NiO nanoparticles before calcination.

The UV–Vis spectra of Cu-doped NiO nanoparticles after calcinations are shown in Fig. 11 that was measured using a USB-2000 UV–Vis spectrophotometer. The absorption edge is observed in the range of 280–350 nm. This blue shift of the absorption edges for different sized nanocrystals is related to the size decrease of particles that is attributed to quantum confinement effect of nanoparticles. The obtained direct optical band gap values 3.75, 3.80 and 3.82 eV for the x = 0.00, x = 0.13 and x = 0.20 samples were determined by Tauc's relation [26]:

$$\alpha h\upsilon = \alpha_0 (h\upsilon - E_g)^{1/2} \quad (2)$$

Where hν, αo and Eg are photon energy, a constant and optical band gap of the nanoparticles, respectively. Absorption coefficient (α) of the powders at different wavelengths can be calculated from the absorption spectra. The values of Eg were determined by extrapolations of the linear regions of the plot of versus. As seen in Fig. 12 and Fig.13, optical band gap values increase with doping concentration increase.

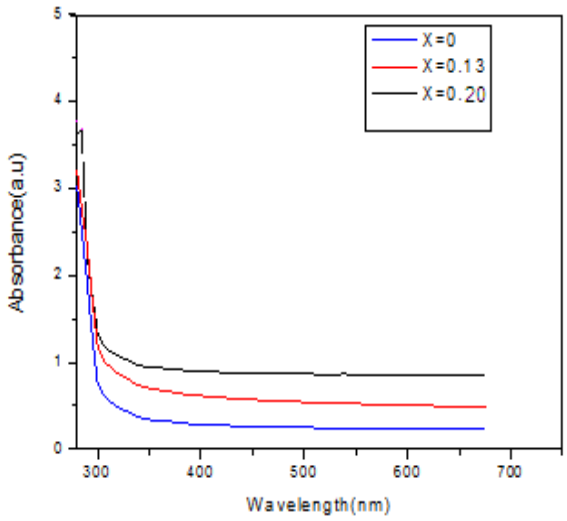

Fig. 11. UV–Vis spectra of Cu-doped NiO nanoparticles after calcination.

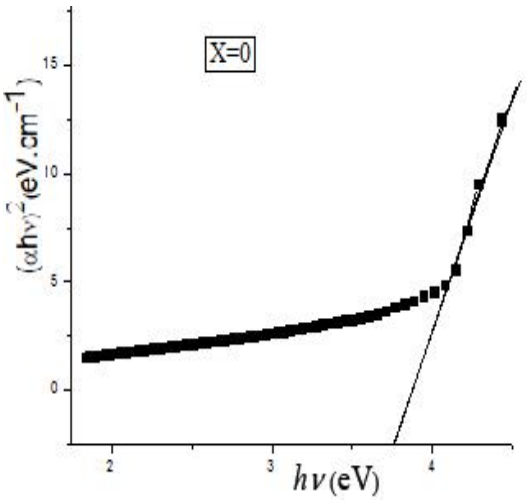

Fig. 12. $(\alpha h\upsilon)^2$ versus $(h\upsilon)$ spectra of x = 0.00 sample.

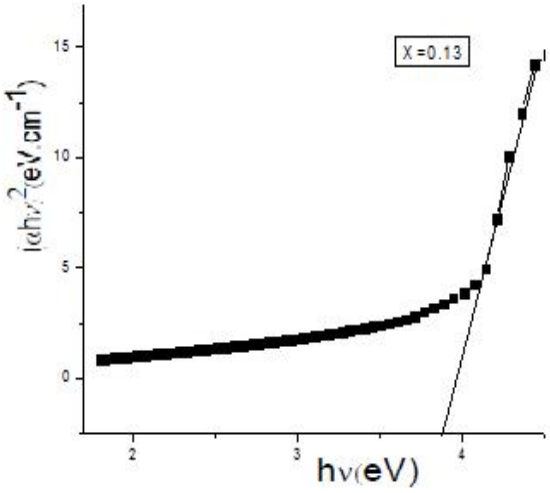

Fig. 13. $(\alpha h\upsilon)^2$ versus $(h\upsilon)$ spectra of x = 0 sample.

Fig. 14 and Fig. 15 show FT-IR spectra taken on JASCO 640 plus infrared spectrometer in the range of 4000–400 cm^{-1} at room temperature. Samples were prepared by mixing powders and KBr, which were ground and pressed into a transparent pellet with a diameter of 1cm. The peaks around 3700 cm^{-1} and 3414 cm^{-1} on the FT-IR spectrum are assigned to be O–H bonds. Absorption at 1632 cm^{-1} attributed to hydroxyl groups. The absorption bonds at 1420 cm^{-1} and 1117 cm^{-1} indicates the existence of carbonates and the bond at 2900 cm^{-1} corresponds to C–H stretching mode [27]. In FT-IR spectrums bonds at 522 cm^{-1} and lower are related to metal oxides vibration bonds. In Cu-doped sample bond at 408 cm^{-1} position probably corresponds to Cu–O vibration bond. The absorption bonds at 454cm^{-1} and 522 cm^{-1} are associated to Ni–O vibration bond [28], but absorption bond at 607 cm^{-1} is assigned to Ni–O–H stretching bond. The above information confirmed formation of pure and Cu-doped NiO nanoparticles. Presence of Carbon impurity in the samples is because of ethanol, which is used for washing.

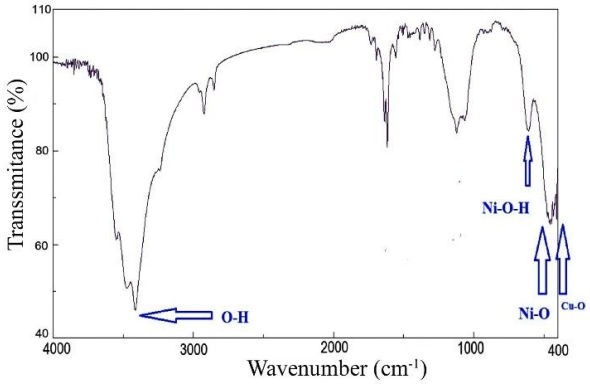

Fig. 14. FTIR spectrum of the x = 0.00 sample after calcinations at room temperature.

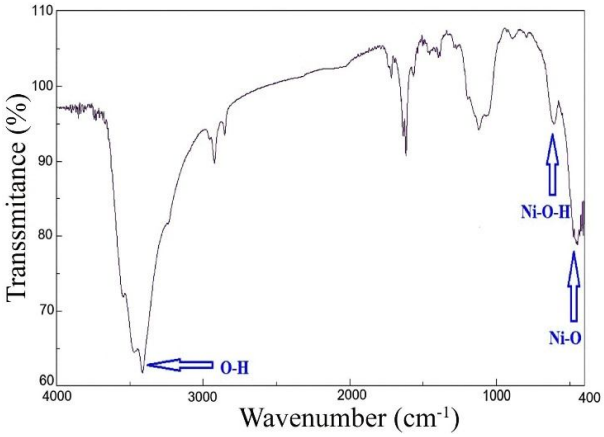

Fig. 15. FT-IR spectrum of the x = 0.13 sample after calcinations at room temperature.

4. Conclusion

The nanoparticles of Cu-doped NiO have been successfully synthesized by a simple co-precipitation method at room temperature. The maximum wavelength absorption appears at

around 280–350 nm, which is because of a blue-shift. It is observed due to an increase in optical band gap when copper doping concentration increases and/or size of particles decreases. XRD analysis showed that the samples prepared are in a cubic phase. The broad peak of XRD pattern indicates nanocrystalline behaviour of particles. The AFM and TEM images confirm that Cu-doped NiO nanoparticles have spherical shape in nanoscale. Study of Magnetic property of samples using VSM technique shows that magnetization of NiO:Cu nanoparticles (after calcinations) increase with Cu doping percentage till 13% , and after x = 0.13, starts decreasing. The FTIR spectrums confirm form of NiO:Cu nanoparticles.

Acknowledgements

The authors would like to thank from University of Sistan and Baluchestan for financial support this work.

References

[1] H. Sato, T. Minami, S. Takata, T. Yamada, Thin solid films. 23 (1993) 27-31.

[2] S.A. El-Molla, M.N. Hammed, G.A. El-Shobaky, Mater. Lett. 58 (2004) 1003-1011.

[3] S.Y. Wu, W.F. Chen, Y.F. Ferng, Mater. Lett. 60 (2006) 790-795.

[4] K.K. Purushothaman, G. Muralidharan, Solar Energy Mater. Solar Cells. 93 (2009) 1195-1201.

[5] Z.G. Liu, Y.G. Zu, Y.J. Fu, Y.L. Zhang, Liang, H.L. Mater. Lett. 62 (2008) 2315-2317.

[6] I. Castro-Hurtado, J. Herran, N. Perez, S.M. Olaizola, G.G. Mandayo, E. Castano, Sens. Lett. 9 (2011) 64-68.

[7] Y. Du, W.N. Wang, X.W. Li, J. Zhao, J.M. Ma, Y.P. Liu, Mater. Lett. 68 (2012) 168-170.

[8] Y. Li, Y.S. Xie, J.H. Gong, Y.F. Chen, Z.T. Zhang, Mater. Sci. Eng. 86 (2001)119-122.

[9] J. A. Borchers, Y. Ijiri, D.M. Lind, P.G. Ivanov, R.W. Erwin, S.H. Lee, C.F. Majkrzak. J. Appl. Phys. 85 (1999) 5883-5885.

[10] Y. Hu, H.S. Qian, T. Mei, J. Guo, T. White, Mater. Lett. 64 (2010) 1095-1098.

[11] V. Biju, Mater. Lett. 62(2008) 2904-2906.

[12] A. C. Gandhi, C.-Y. Huang, C. C. Yang, Ting S. Chan, C.-L. Cheng, Y.-R. Ma, S. Y. Wu, Nanoscale Res. Lett. 6 (2011) 485-503.

[13] W. Shin, N. Murayama, Mater. Lett. 45 (2000) 302-306.

[14] H. Sato, T. Minami, S. Takata, T. Yamada, Thin Solid Films. 236 (1993) 27-31.

[15] Q.X. Xia, K.S. Hui, K.N. Hui, D.H. Hwang, S.K. Lee, W. Zhou, Y.R. Cho, S.H. Kwon, Q.M. Wang, Y.G. Mater. Lett. 69 (2012) 69-71.

[16] W. Guo, K.N. Hui, K.S. Hui, Mater. Lett. 92 (2013) 291-295.

[17] L. Xiang, X.Y. Deng, Y. Jin, Scr. Mater. 47 (2002) 219-224.

[18] Y.D. Wang, C.L. Ma, X.D. Sun, H.D. Li, Chem. Commun. 5 (2002) 751-755.

[19] Tao Dongliang, Wei Fei, Mater. Lett. 58 (2004) 3226-3228.

[20] I.W. Lenggoro, Y. Itoh, N. Iida, K. Okuyama, Mater. Res. Bull. 38 (2003) 1819-1827.

[21] .D. Wang, C.L. Ma, H.D. Li, Inorg. Chem. Commun. 5 (2002) 751-755.

[22] C.B. Wang, G.Y. Gau, S.J. Gau, C.W. Tang, J.L. Bi, Catal. Lett.101 (2005) 241-247.

[23] D. Tao, F. Wei, Mater. Lett. 58 (2004) 3226-3228.

[24] S.I. Cherrey, O. Tillement, J.M. Dubois, F. Massicot, Y. Fort, J. Ghanbaja, S.B. Colin, Mater. Sci. Eng. A. 338 (2002) 70-75.

[25] S. Kumar , Y.J. Kim , B.H. Koo, C.G. Lee, Journal of Nanoscience and Nanotechnology. 10 (2010) 7204-7207.

[26] J. Tauc, The optical constants are determined by three methods; one of them is new and Properties of Solids, Academic Press, Inc**.** New York**,** 1966.

[27] A.Sharma, P. S. Kumar, S. Dahiya , N. Budhiraja, Adv. Appl. Sci. Res. 4 (2013) 124-130.

[28] F. Davar, Z. Fereshteh, M. Salavati-Niasari, J. Alloys Compd. 476 (2009) 797-801.